JMEPEG (2021) 30:2545–2551
https://doi.org/10.1007/s11665-021-05588-5

1059-9495/$19.00

On the Relation Between Pressing Energy and Green Strength at Compaction of Hard Metal Powders

Kristin Salmi, Hjalmar Staf, and Per-Lennart Larsson

Submitted: 3 November 2020 / Revised: 4 January 2021 / Accepted: 12 February 2021 / Published online: 9 March 2021

The relation between pressing energy and green strength is examined experimentally and numerically using a commercially available design of experiment (DOE) software, at compaction of five hard metal powder materials. This is of substantial practical importance, in particular at pressing of complicated geometries when high values on the green strength is necessary. The compaction energy is here experimentally determined at uniaxial compaction of a cylindrical die, filled with powder material, by measuring punch force and compression. The corresponding measurements of the resulting green strength are performed using standard three-point bend (3PB) testing. The statistical analysis of the results shows that the relation between the two properties, pressing energy and green strength, is very close to a linear fit with the coefficient of determination R^2 taking on the value 0.92. This suggests that the pressing energy is an important quantity for reaching a target value on the green strength and the linear relation is certainly convenient in particular when compaction of similar materials is at issue. In parallel with the experimental work finite element calculations are performed in order to evaluate the effect from friction between the powder and the die wall, and it was found that this feature has a limited effect on the pressing energy when similar materials are at issue and is not detrimental for the usefulness of the present correlation approach.

Keywords cemented carbide powders, correlation, cylindrical die, green strength pressing energy, pressing energy, three-point bend testing

1. Introduction

In manufacturing of cutting tool inserts, powder metallurgy is a commonly used method. Cemented carbide powder is compacted to a desired shape using a tool specifically designed for the purpose, which results in a part close to the finished shape that after sintering requires none to very little machining. Investigating a powder by pressing and sintering can be a time consuming and costly process. Therefore, to be able to predict the compaction behavior based on measurements that can be performed earlier on or in less time would thus be beneficial.

The strength of the green body (the green strength) is a central quantity during the compaction process. In an industrial situation, after pressing the green body, it is moved to a sintering plate using a robot. It is clear that for such a process to be successful a sufficiently high green strength is required. As the current industrial trend is directed toward more complicated geometries, it becomes even more important to create green bodies with sufficiently high strength.

Modeling is a very important tool when it comes to predicting the compaction behavior and relevant material quantities. This concerns both macro- and micromechanical modeling where in the first case macroscopic constitutive models are at issue and powder compaction to high density is treated phenomenologically assuming a porous solid. When analyzing cemented carbide powder materials most often a Drucker–Prager CAP model (Ref 1-3) is used. In a micromechanical approach either analytical (Ref 4) or numerical methods, such as the discrete element method (DEM) (Ref 5-9), are of interest. In Ref 6 and Ref 7, DEM simulations are compared with experiments and it is concluded that the numerical results are accurate up to material densities being approximately 50%–60% of a fully compacted insert, which evidently is not sufficient for simulation of the entire manufacturing process.

Mechanical modeling of powder compaction relies heavily on high quality experimental results. Such testing can, however, be cumbersome and expensive, and it is important that the experimental results can be presented in a general form. This is so both for practical purposes in an industrial situation and as input to mechanical models. Therefore, it would be interesting to see whether there exists a relevant correlation between properties pertinent to determination of the green strength. Accordingly, this is the matter of interest in the present investigation with focus on the relation between pressing energy and green strength.

For this purpose, five different tungsten carbide powder materials are produced with varying amount and hardness of the pressing agent (PEG). The powders as well as their resulting pressed green bodies are subjected to testing in order to characterize their properties; and in particular in this work, pressing energy and green body strength. These two properties are of direct importance during production but also as input to the above discussed macro- and micromechanical modeling attempts (as already indicated above). Consequently, the testing includes powder compaction in a cylindrical die and green body bending properties (strength). All results are then statistically evaluated using the design of experiment (DOE)

Kristin Salmi and **Per-Lennart Larsson**, Department of Engineering Mechanics, Unit of Solid Mechanics, Royal Institute of Technology (KTH), 10044 Stockholm, Sweden; and **Hjalmar Staf**, Sandvik Coromant, 126 80 Stockholm, Sweden. Contact e-mail: hjalles@kth.se.

software Modde 12 (Ref 10) with the purpose of finding correlations between measurements on different powders.

In parallel with the experimental work finite element calculations are performed in order to determine the influence from friction on the results and conclusions. The finite element calculations rests on a Drucker–Prager CAP model first presented for powder material analysis in Ref 1 and further developed as regards the constitutive description in Ref 3. As for the frictional behavior at powder/die wall contact, this has been studied substantially in the literature (Ref 11-18) with all these investigations relying on different versions of Coulomb friction. In the present finite element analysis, the friction models presented in Ref 12 and 18 are relied upon.

2. Material and Methods

2.1 Material

The cemented carbide powder that is used in this study consists of approximately 88 wt.% tungsten carbide (WC), 10 wt.% cobalt (Co), 2 wt.% pressing agent (polyethylene glycol, PEG), and 0.5 wt.% alloys. The amount of PEG is however varied in the investigation as specified below. The particle sizes of the raw materials are typically 0.8 µm. The spray drying process creates spherical particles with a diameter of approximately 100 µm, which make up the powder. A typical microstructure of the resulting powder assembly is shown in Fig. 1 at different stages of sieving.

Tungsten carbide (WC) is a hard metal compound used because of its high hardness and stiffness, making it suitable in cutting and milling applications with high forces. To further resist fracture, it is combined with a bonding material which keeps the material together and increases the toughness. In this case, cobalt (Co) is used as the bonding material. The carbide powder also contains some alloys, for instance chromium carbide which is used to deaccelerate grain growth during sintering.

In order to achieve a variation of the properties of the cemented carbide after compaction the PEG amount is varied according to Table 1 (note that the PEG molar mass is also varied). It should be noted in passing that the pressing agent (PEG) is added to hold the compacted green body together before the sintering. It also increases the flowability of the powder which is necessary during compaction for filling properly. During sintering, the pressing agent is decomposed, leaving only the cemented carbide in the finished insert.

2.2 Measurements

In this investigation two types of measurements are carried through. The material mixtures for the tungsten carbide powder used in both experiments are of course the same, with, as mentioned above, the PEG amount being varied according to Table 1 (note that the PEG molar mass is also varied).

In the first and initial measurement type uniaxial compaction (compression) of a cylindrical die is performed in order to produce green bodies of the five different materials described above and to determine the pressing energy. The cylindrical die used has been developed and described previously in Ref 19 and (20) and is also shown schematically in Fig. 2. This is a multiple purpose experimental device where also contact pressures p_i along the die wall as well as frictional forces can be determined for the purpose of constitutive characterization and description of the frictional behavior. For the present analysis, only F_{UP} (force on the upper punch) is of interest.

The energy uptake is calculated for every pressing sequence up until unloading. The energy is defined as

$$W = \int F_{\mathrm{UP}} \mathrm{d}x \qquad \text{(Eq 1)}$$

, where F_{UP} is, as already mentioned above, the force on the upper punch and x is the compression of the powder material

Table 1 Powder labels, amount [wt.%] of PEG, hardness of PEG (qualitative) and molar mass of PEG (qualitative)

Name	PEG amount [wt.%]	PEG hardness	PEG molar mass
S 1.5	1.5	Soft	Small
H 2.5	2.5	Hard	High
M 2.0	2.0	Medium	Medium
S 2.5	2.5	Soft	Small
H 1.5	1.5	Hard	High

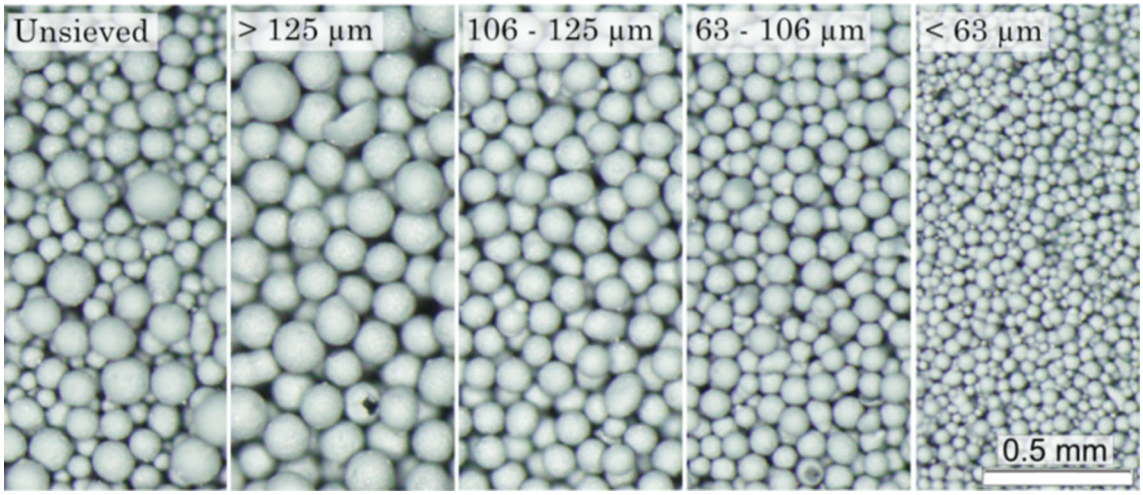

Fig. 1 Typical powder assembly after different stages of sieving

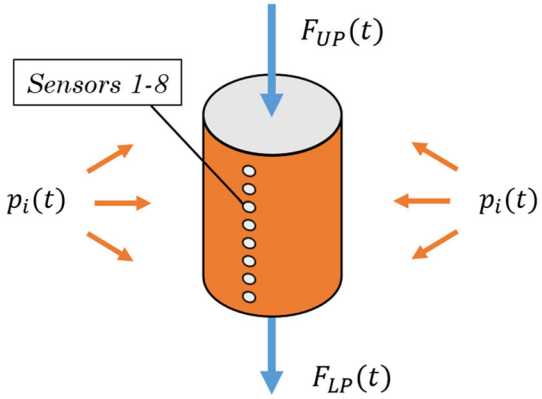

Fig. 2 Free body diagram of the instrumented die compaction test. This is a multiple purpose experimental device where also contact pressures p_i along the die wall, recorded by an individual sensor i, as well as frictional forces can be determined for the purpose of constitutive characterization and description of the frictional behavior. For the present analysis only F_{UP} (force on the upper punch) is of interest. Note that t denotes natural time

cylinder. The difference between F_{UP} and F_{LP}, force on the lower punch, is due to frictional effects. For calculating the energy, the maximum force is set for every pressing such that the relative density ρ_{rel} is held constant. The relative density is defined as follows:

$$\rho_{\mathrm{rel}} = m_p/\left(\rho_s \pi r^2 h\right) \qquad \text{(Eq 2)}$$

, where m_p is the powder mass, ρ_s is the fully sintered density, r is the die radius and h is the height of the compacted specimen. Presently m_p, ρ_s, and r are known and h is chosen in order to achieve a relative density being 0.5 (indicating that the density will double after sintering).

For testing of the green strength, green body cuboid pieces are pressed with a geometry according to Fig. 3(a), with measurements $B = 6.025$ mm, $H = 6.245$ mm, and $L = 25$ mm. The specimens are pressed up to a relative density being 0.5 in order to ensure a proper comparison with the pressing energy results described above. The test specimens are subject to a 3PB testing, as shown in Fig. 3(b), where the green body is placed on two support pins and centered with respect to the loading pin. The loading pin then moves in a vertical direction until the body cracks. The test is repeated three times for every type of powder.

From the test, the stress as a function of the flexural strain is recorded. The fracture stress σ_B is calculated based on standard engineering beam theory assuming elastic material behavior, according to

$$\sigma_B = 3F_B l/\left(2BH^2\right) \qquad \text{(Eq 3)}$$

In (3), F_B is the applied bending force at fracture and $l = 20$ mm is the length between the support pins.

2.3 Finite Element Analysis

A feature that could influence the present analysis in a negative manner is frictional effects between powder and die wall. This is a particularly troublesome issue as the presence of frictional forces will indeed have an influence on the pressing energy, but this part of the energy will not contribute to the compaction of the powder material (and thereby the green strength).

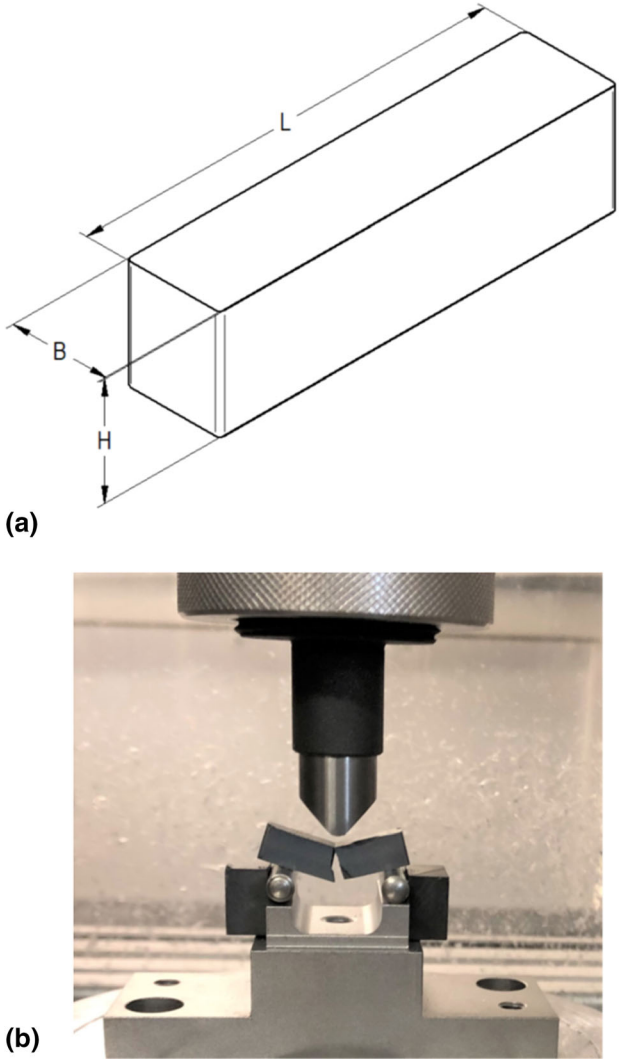

Fig. 3 Geometry and test setup for the three-point bending test. (a) Geometry of a cuboid piece used for 3PB. (b) The cuboid piece setup in the load cell for the 3PB test. Picture taken after test ending

In order to investigate this issue finite element simulations of cylindrical die powder compaction were performed including frictional effects. Similar simulations have been carried through elsewhere, cf., e.g., (Ref 3), and for the details of the finite element approach, this study is referred to. In the simulations, a cemented carbide powder material is investigated. This material is of course similar to the ones investigated experimentally here. The material model used in the simulations is a Drucker–Prager CAP model, as originally proposed in Ref 21 and specified for powder materials (Ref 1) with, among other things, density dependent constitutive properties. Other relevant applications of such a constitutive equation to powder materials can be found in for example (Ref 2, 3) and (Ref 22). Explicit values on the presently used constitutive quantities are listed in (Ref 3).

All the finite element simulations are performed using the general-purpose finite element program LS-Dyna (Ref 23, 24). Explicit time integration is utilized but quasi-static conditions are ensured by a low pressing rate. The cylindrical die geometry

has already been schematically shown in Fig. 2 and discretization of the powder material in the die is shown in Fig. 4. The final value on the material relative density is varying due to frictional effects but on average slightly it takes on a value slightly above 0.5.

The two versions of the frictional behavior implemented in the finite element model are specified in Ref 12 and 18. The first one as presented in Ref 12 is a standard one for cemented carbide powders where the friction coefficient in Coulombs friction law, μ, is set to a constant value. According to Ref 12,

$$\mu = 0.2. \quad \text{(Eq 4)}$$

The other one presented in Ref 18, also pertinent to cemented carbide powders, is a more advanced model where it is recognized that the frictional coefficient will depend on the contact pressure between powder and die wall. Utilizing the cylindrical die with pressure sensors shown in Figure 2, it was possible in Ref 18 to determine the average pressure dependent friction coefficient and the results are shown in Figure 4. Obviously, these results are very different from Eq. (4) even though it should be noted that at high pressure values (the final stages of pressing) $\mu = 0.2$ is a very good approximation. The experimental curve in Figure 4 was then modeled in (Ref 18) by assuming a local pressure dependent friction coefficient

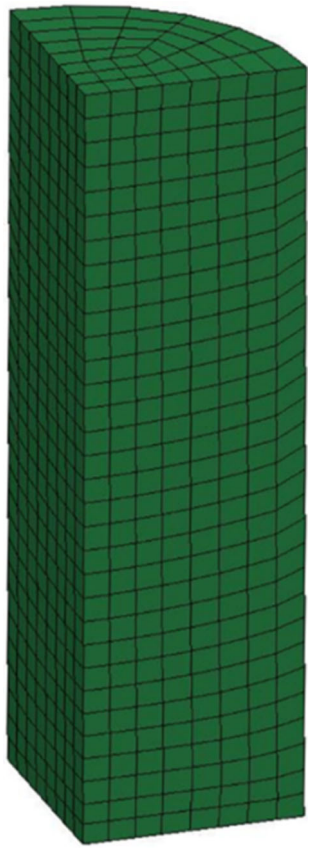

Fig. 4 FE model used in the current analysis. The powder material is marked in green and modeled with solid elements with discretization according to the figure. Two symmetry planes are introduced in order to reduce the number of elements used in the simulations. Because of limitations in LS-Dyna, the cylinder could not be modeled as axisymmetric

$$\mu_{\text{opt}} = \begin{cases} a_1 + a_2 \cdot p & \text{if} \quad p < p_1 \\ a_3 & \text{if} \quad p_1 \le p \le p_2 \\ (p/a_4)^{-a_5} & \text{if} \quad p > p_2 \end{cases} \quad \text{(Eq 5)}$$

with explicit parameter values

$$a_1 = -0.036;\ a_2 = 0.48\ \text{MPa}^{-1};\ a_3 = 0.49;\ a_4 = 0.30\ \text{MPa};\ a_5 = 0.33 \quad \text{(Eq 6)}$$

and stress parameters

$$p_1 = 1.1\ \text{MPa};\ p_2 = 2.5\ \text{MPa}. \quad \text{(Eq 7)}$$

yielding very good agreement between experiments and theory/numerics as shown in Fig. 5.

Presently then, finite element simulations of cylindrical die compaction were performed in order to determine the pressing energy pertinent to the two friction models in Eq. (4) and (5). It should be mentioned that numerical implementation of the two friction models into LS-Dyna (Ref 23, 24) have been discussed in detail in Ref 25.

3. Results and Discussion

In this section, the experimental results pertinent to the pressing energy and the green strength measurements are presented separately. After that, results related to the correlation between these properties are presented. In the latter case, as mentioned above, the design of experiment (DOE) software Modde 12 (Ref 10) is used. Finally, based on the finite element results frictional effects are evaluated and discussed in relation to correlation.

3.1 Pressing Energy Results

The pressing energy during compaction show clear differences between the five different powders as tabulated in Table 1. In Fig. 6, averages of all powders are depicted in order

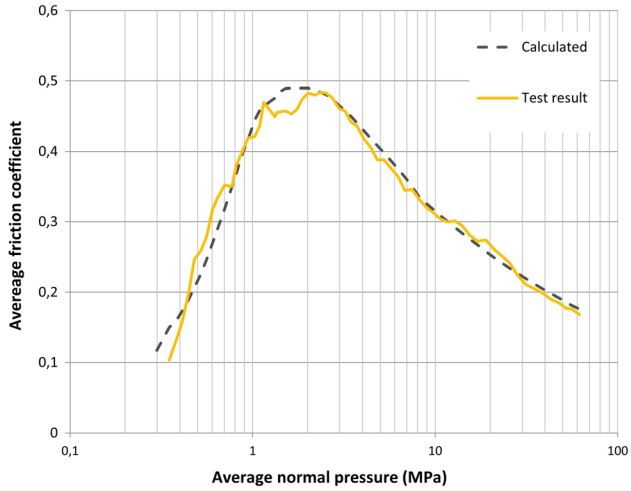

Fig. 5 Average frictional coefficient over the whole cylindrical die powder pillar is shown. The yellow curve is determined directly from test results and the gray curve is calculated using Eq. (5). The results are taken from [26]

to illustrate the difference. Note that the curves are normalized so that unloading occurs at $t = 0$ s.

The difference between the largest and the smallest pressing energy, at the end of compaction, is found to be approximately 42%. The highest values are found for hard and high amount PEG.

It should be emphasized once again that compaction is continued until the relative density of powder material is 0.5. Corresponding comparisons at other values on the relative density can be made from the results in Fig. 6 but are not detailed here.

3.2 Green Strength Results

The green strength is as mentioned above determined by a three-point bending test, where the maximal force prior fracture is recorded. The green strength (fracture stress) is then determined from Eq. (3). Figure 7 shows the results of the bending tests, where the fracture stress is plotted against the strain prior to fracture. Note that the strain, as well as the fracture stress in Equation (3), is determined according to standard engineering beam theory.

The test results show large differences for the different PEG types. It can be seen that the powder H 2.5 endures significantly higher loads compared to the other powders. It can also be seen that the harder the PEG type in the powder is, the higher the fracture stress becomes.

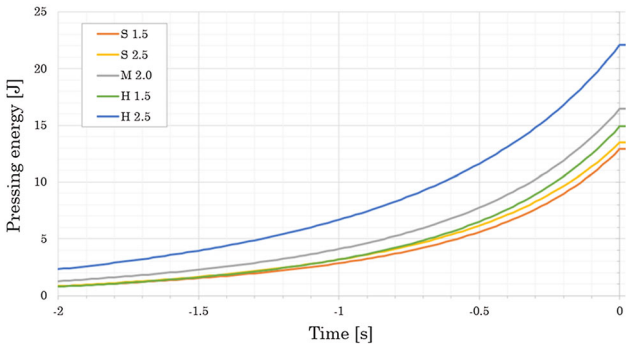

Fig. 6 Average pressing energy curves for each powder, normalized so that unloading occurs at time $t = 0$ s

It should be mentioned that in the green strength analysis simplifications are made concerning the evaluation. As mentioned above standard engineering beam theory is used to determine fracture stress and strain which consequently limits the analysis to elastic material behavior. From inspection of the bending test output, it can be concluded however that this is a satisfactory assumption as very little nonlinearities are found. Furthermore, only correlation of the properties is at issue and highly accurate strength results are relevant but not of highest importance.

3.3 Correlation Results

Correlation between the two properties is tested using so called multiple linear regression (MLR) remembering that in this case two response variables are at issue. The analysis is as previously mentioned performed using the design of experiment (DOE) software Modde 12 (Ref 10). Correlation is presently determined based on the coefficient of determination R^2. R^2 takes on values between 0 and 1, where 1 indicates perfect correlation between the quantities at issue.

The results from the analysis are depicted as a scatter plot in Fig. 8. Clearly, the results are very well fitted to a linear curve (as also indicated in Fig. 8). The R^2-coefficient for a linear fit takes on the value 0.92 indicating very good correlation.

It should be emphasized that it is not altogether surprising that there is a strong correlation between the two investigated quantities. If an insert requires a large amount of energy to be compacted into a certain density, it could be expected that the insert also is stronger and performs better in a strength test. What is surprising, however, is that this linear correlation is so good despite of the fact that quite different materials are included in the investigation.

3.4 Finite Element Results

The results from the finite element simulations are depicted in Fig. 8. Obviously the two sets of results differ since the two

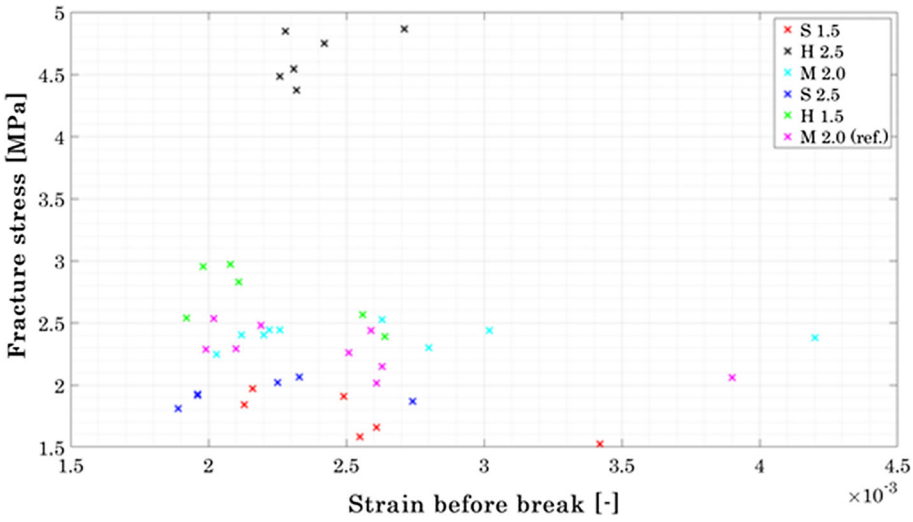

Fig. 7 Results of the three-point bending test measurements. The markers correspond to each test's breaking point and show a clear difference for the different PEG types where harder PEG correlates to higher stress prior rupture. Note that M 2.0 (ref) is the same material as M 2.0 but manufactured at a different site in order to ensure generality of the results

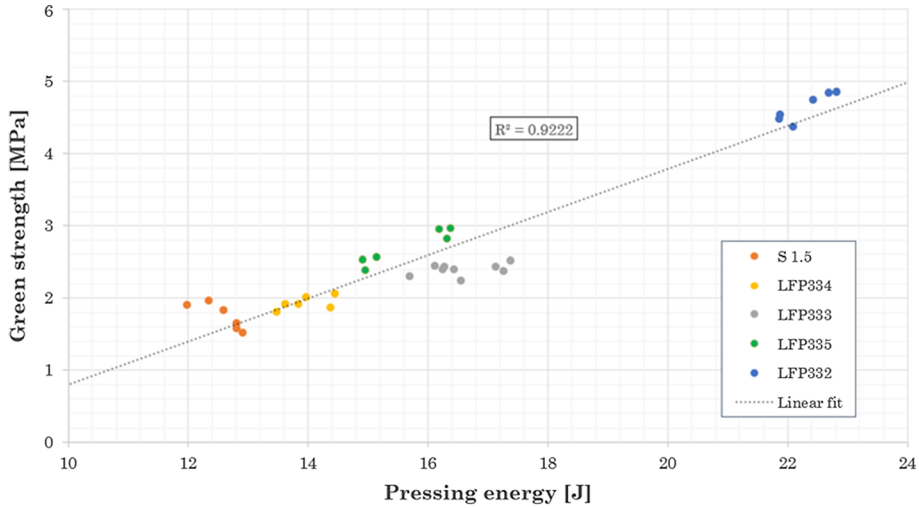

Fig. 8 Correlation between pressing energy W and the green strength for each powder

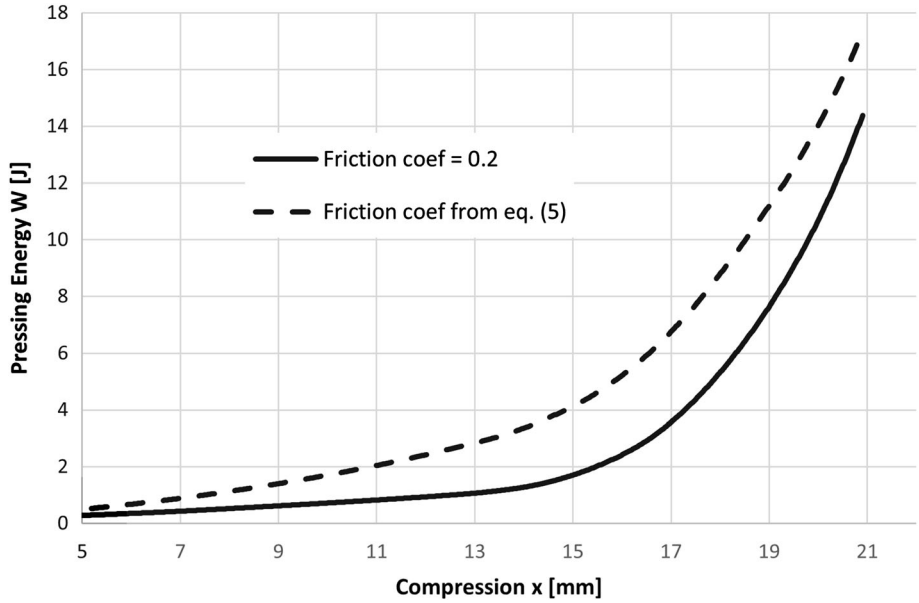

Fig. 9 Pressing energy W as function of compression x for the two frictional descriptions in Eqs. (4) and (5). Finite element results based on the constitutive model specified in (Ref 3)

frictional descriptions in Eqs. (4) and (5) are very different. At higher compaction pressure, however, both frictional models yield approximately the same value on the friction coefficient and clearly, since results at higher pressure are the major contributor to the integral value in Eq. (1), the two sets of results start to get much closer.

It should be emphasized that the two frictional models in Eqs. (4) and (5) are very different (representing a worst-case scenario) and in short, they are pertinent to the frictional behavior of two quite different powder materials. For similar materials, such as the ones studied here, deviating effects from friction on the pressing energy would be much smaller than what is shown in Fig. 9. Accordingly, it can be concluded from the finite element results that for the materials at issue presently, frictional effects will have a very small influence on the very good correlation, between the two quantities at issue as reported above.

4. Conclusions

Correlation between the powder material properties granule strength and green strength was investigated experimentally and numerically using a design of experiment (DOE) software. The investigation was pertinent to cemented carbide powder materials. In order to achieve a variation of the properties of the cemented carbide after compaction the PEG (pressing agent) amount and molar mass was varied.

It is found that the correlation between the two quantities is very good with the R^2-coefficient for a linear fit taking on the

value 0.92. From a physical point of view good correlation is perhaps not surprising as it could be expected that an insert pressed with high energy also is stronger and performs better in a strength test. The very high degree of correlation is however surprising.

Possible frictional effects on the results are investigated and it is concluded that this feature will only slightly affect the difference in pressing energy for similar materials. Accordingly, such effects can be disregarded when applying the present approach when cemented carbide powders are at issue.

From a practical point of view the results are of substantial importance at pressing of complicated geometries when high values on the powder material green strength is necessary. The results suggest that it is possible to get information about one material by experimentally characterizing another one which is a valuable finding for many types of powder materials. A possible continuation of the present research would be to investigate how the residual porosity of the material after sintering is depending on the pressing energy. Such results should be supported with microscopic data.

Funding

Open access funding provided by Royal Institute of Technology.

Open Access

References

1. J. Brandt and L. Nilsson, A Constitutive Model for Compaction of Granular Media with Account for Deformation Induced Anisotropy, *Mech. Cohesive Frict. Mater.*, 1999, **4**, p 391–418
2. H. Staf, D.C. Andersson, P. Lindskog and P.-L. Larsson, On the influence of Material Parameters in a Complex Material Model for Powder Compaction, *J. Mater. Eng. Perform.*, 2016, **25**, p 4408–4415
3. H. Staf, E. Olsson and P.-L. Larsson, Mechanical characterization of Powder Materials: A General Approach Detailed for Cemented Carbides, *Powder Technol.*, 2020, **364**, p 531–537
4. B. Storåkers, N. Fleck and R. McMeeking, The Viscoplastic Compaction of Composite Powders, *J. Mech. Phys. Solids*, 1999, **47**, p 785–815
5. C.L. Martin and D. Bouvard, Study of the Cold Compaction of Composite Powders by the Discrete Element Method, *Acta Mater.*, 2003, **51**, p 373–386
6. E. Olsson and P.-L. Larsson, A Numerical Analysis of Cold Powder Compaction Based on Micromechanical Experiments, *Powder Technol.*, 2013, **243**, p 1185–1201
7. E. Olsson and P.-L. Larsson, Micromechanical Investigation of the Fracture Behavior of Powder Materials, *Powder Technol.*, 2015, **286**, p 288–302
8. B. Harthong, J.-F. Jerier, P. Doremus, D. Imbault and F.-V. Donze, Modeling of High Density Compaction of Granular Materials by the Discrete Element Method, *Int. J. Solids Struct.*, 2009, **46**, p 3357–3364
9. B. Harthong, J.-F. Jerier, V. Richefeu, B. Chareyre, P. Doremus, D. Imbault and F.-V. Donze, Contact Impingement in Packings of Elasticplastic Spheres, Application to Powder Compaction, *Int. J. Mech. Sci.*, 2012, **61**, p 32–43
10. Umetrics. Modde. Version 12.0.0.3292. https://umetrics.com
11. S. Strijbos, Powder-Wall Friction: The Effects of Orientation of Wall Grooves and Wall Lubricants, *Powder Technol.*, 1977, **18**, p 209–214
12. P. Samuelsson and B. Bolin, Experimental Studies of Frictional Behavior of Hard Metal Powder Sliding on Cemented Carbide Walls, *Scand. J. Metall.*, 1983, **12**, p 315–322
13. J.G. Wagner, The Frictional Behavior of Tungsten and Molybdenum Powders Sliding on Die Materials, *Powder Technol.*, 1983, **35**, p 47–50
14. B.J. Briscoe and S.L. Rough, The Effects of Wall Friction in Powder Compaction, *Colloids Surf. A*, 1998, **137**, p 103–116
15. B. Wikman, N. Solimannezhad, R. Larsson, M. Oldenburg and H.-A. Häggblad, Wall Friction Coefficient Estimation Through Modelling of Powder Die Pressing Experiment, *Powder Metall.*, 2000, **43**, p 132–138
16. I.M. Cameron and D.T. Gethin, Exploration of Die Wall Friction for Powder Compaction Using a Discrete Finite Element Modelling Technique, *Modell. Simul. Mater. Sci. Eng.*, 2001, **9**, p 289–307
17. D.M.M. Guyoncourt, J.H. Tweed, A. Gough, J. Dawson and L. Pater, Constitutive Data and Friction Measurements of Powders Using Instrumented Die, *Powder Metall.*, 2001, **44**, p 25–33
18. H. Staf, E. Olsson, P. Lindskog and P.-L. Larsson, Determination of the Frictional Behavior at Compaction of Powder Materials Consisting of Spray-Dried Granules, *J. Mater. Eng. Perform.*, 2018, **27**, p 1308–1317
19. D.C. Andersson, P. Lindskog and P.-L. Larsson, Inverse Modeling Applied for Material Characterization of Powder Materials, *J. Test. Eval.*, 2015, **43**, p 1005–1019
20. P. Lindskog, D.C. Andersson and P.-L. Larsson, An Experimental Device for Material Characterization of Powder Materials, *J. Test. Eval.*, 2013, **41**, p 504–516
21. F.L. DiMaggio and I.S. Sandler, Material Model for Granular Solids, *J. Eng. Mech. Div. ASCE*, 1971, **96**, p 935–950
22. P. Jonsen and H.-Å. Häggblad, Modelling and Numerical Investigation of Residual Stress State in Green Metal Powder Body, *Powder Technol.*, 2005, **155**, p 196–208
23. J.O. Hallqvist, *LS-Dyna Theory Manual*, Livermore, California, USA, 2006
24. LS-Dyna keyword user's manual II, material models, Livermore, California, USA, 2018
25. H. Staf and P.-L. Larsson, Evaluation of an Advanced Powder-Die Frictional Model, *Powder Technol.*, 2020, **363**, p 569–574